J. Biochem. **139**, 591–596 (2006)
doi:10.1093/jb/mvj057

Catalytic Promiscuity in Dihydroxy-Acid Dehydratase from the Thermoacidophilic Archaeon *Sulfolobus solfataricus*

Seonghun Kim[1,2] and Sun Bok Lee[1,2,3,*]

[1]School of Environmental Science and Engineering, [2]Division of Molecular Life and Sciences, and 3Department of Chemical Engineering, Pohang University of Science and Technology, San 31, Hyoja-dong, Pohang 790-784, Korea

Received October 18, 2005; accepted January 25, 2006

Dihydroxy-acid dehydratase (DHAD) is one of the key enzymes involved in the biosynthetic pathway of the branched chain amino acids. Although the enzyme has been purified and characterized in various mesophiles, including bacteria and eukarya, the biochemical properties of DHAD from hyperthermophilic archaea have not yet been reported. In this study we cloned, expressed in *Escherichia coli*, and purified a DHAD homologue from the thermoacidophilic archaeon *Sulfolobus solfataricus*, which grows optimally at 80°C and pH 3. The recombinant *S. solfataricus* DHAD (rSso_DHAD) showed the highest activity on 2,3-dihydroxyisovalerate among 17 aldonic acids tested. Interestingly, this enzyme also displayed high activity toward D-gluconate and some other pentonic and hexonic sugar acids. The k_{cat}/K_m values were 140.3 mM^{-1} s^{-1} for 2,3-dihydroxyisovalerate and 20.0 mM^{-1} s^{-1} for D-gluconate, respectively. A possible evolutionary explanation for substrate promiscuity was provided through amino acid sequence alignments of DHADs and 6-phosphogluconate dehydratases from archaea, bacteria and eukarya.

Key words: dihydroxy-acid dehydratase, evolution of metabolism, gluconate dehydratase, 6-phosphogluconate dehydratase, substrate promiscuity, *Sulfolobus solfataricus*.

Abbreviations: DHAD: dihydroxy-acid dehydratase; EDD: 6-phosphogluconate dehydratase; GNAD: gluconate dehydratase.

Dihydroxy-acid dehydratase (DHAD, 2,3-dihydroxy-acid hydrolyase, EC 4.2.1.9) catalyzes the dehydration of 2,3-dihydroxyisovalerate and 2,3-dihydroxy-3-methylbutyrate to produce 2-keto-isovalerate and 2-keto-3-methylbutyrate, respectively (*1*). This enzyme plays a role in the biosynthesis of the branched-chain amino acids valine and isoleucine in organisms ranging from archaea and bacteria to eukarya. Until now, several DHADs have been purified and characterized from bacteria (*2–5*) and eukarya (*6–8*), but not from archaea.

DHAD belongs to the ILVD_EDD protein family (Pfam00920). Two dehydratases, DHAD and 6-phosphogluconate dehydratase (EDD), have been shown to be evolutionarily related, and a comparison of their amino acid sequences showed that they are highly homologous (*9*, *10*). Biochemical studies of DHADs indicate that these enzymes have similar properties. DHAD is usually a dimer consisting of identical subunits ranging from 62 to 66 kDa. Its enzyme activity is optimal at pH values around 8, is enhanced in the presence of divalent metal ions, and is inhibited by heavy metal ions, fluorides, and chelating agents (*2–8*). EDD catalyzes the first step in the Entner-Doudoroff pathway, the dehydratation of 6-phosphogluconate into 2-keto-3-deoxy-6-phosphogluconate. *E. coli* EDD enzymes share 54% homology with *E. coli* DHAD, and the two enzymes (EDD and DHAD) are activated by divalent cations such as Fe^{2+}, Mn^{2+}, and Mg^{2+} (*9*, *10*). In addition to these enzymes, bacterial gluconate dehydratase (GNAD) displays properties similar to EDD and DHAD. For example, GNAD from *Clostridium pasteurianium* (*11*, *12*), which catalyzes the dehydration of non-phosphorylated gluconate to 2-keto-3-deoxy-gluconate, is a dimer consisting of identical subunits of 64 kDa with an optimum pH of 7.3–7.8 and is activated by divalent cations such as Fe^{2+}. It is believed, based on the biochemical properties of EDD, DHAD, and GNAD, that these enzymes are probably closely related.

Recently, Danson and his coworkers (*13*, *14*) reported that three enzymes of the glycolysis pathway of *Sulfolobus solfataricus* (glucose dehydrogenase, gluconate dehydratase, and 2-keto-3-deoxy-gluconate aldolase) exhibited a catalytic promiscuity that enables them to be used for the metabolism of both glucose and galactose. This led us to investigate the possibility of catalytic promiscuity in *S. solfataricus* DHAD. Although DHADs have been purified and characterized in various bacteria and eukarya, the properties of DHAD from archaea have not been previously reported. In this work, we describe the cloning of the *ilvD* gene encoding DHAD from the hyperthermophilic archaeon *S. solfataricus* and the characterization of the recombinant enzyme expressed in *E. coli*. Our results indicate that *S. solfataricus* DHAD exhibits substrate promiscuity with a high activity toward D-gluconate and D-xylonate.

*To whom correspondence should be addressed. Tel: +82-54-279-2268, Fax: +82-54-279-5528, E-mail: sblee@postech.ac.kr

MATERIALS AND METHODS

Cloning, Expression, and Purification of DHAD—The genomic DNA of *S. solfataricus* (DSM1617) was prepared as described previously (*15*). The manipulations of plasmid DNA from *E. coli* were carried out by standard methods (*16*). The *ilvD* gene, encoding a DHAD, was amplified by PCR using *S. solfataricus* genomic DNA as the template, with Taq DNA polymerase (Takara, Otsu, Japan), and two primers (forward primer, 5′-ACTGCAGATGCCAGCAAAATTAAATAGTCCC-3′ and reverse primer, 5′-GGAATTCAAATTAAGCTGGTCTAGTCACAG-3′). The primers included restriction sites (underlined) for *Pst*I and *EcoR*I upstream and downstream, respectively, from the initiation site. A 1,674-bp fragment of *ilvD*, encoding a DHAD from *S. solfataricus*, was amplified by PCR from genomic DNA and cloned into the plasmid pBAD/HisA (Invitrogen), yielding pBAD-Sso_ilvD. *E. coli* TOP10 harboring pBAD-Sso_ilvD was cultivated in LB medium supplemented with 100 μg/ml of ampicillin at 37°C until the optical density at 600 nm reached 0.4–0.6, and then 20% L-arabinose was added to the culture broth to induce gene expression. After induction for 5 h, the cells were harvested. The recombinant cells were resuspended in 50 mM Tris-HCl (pH 7.2) and were disrupted by sonication. The crude extracts were heated at 90°C for 20 min, and the heat-denatured proteins and cell debris were removed by centrifugation (50,000 × *g*, 1 h, 4°C). The clarified homogenate was loaded onto a Ni-NTA column (2.5 × 10 cm) previously equilibrated with 50 mM Tris-HCl (pH 7.2) and was eluted with three bed volumes of the buffer, followed by a linear gradient of 0.0–0.5 M imidazole. Fractions of 3 ml were collected at a flow rate of 0.5 ml/min. Those fractions containing DHAD activity were pooled, concentrated using a Vivaspin concentrator membrane (Vivascience, Lincoln, UK), and loaded onto a Superose 12 column (1.0 × 30 cm) equilibrated with 50 mM Tris-HCl buffer (pH 7.2) containing 0.3 M NaCl. The enzyme was eluted using the same buffer at 0.1 ml/min. The active fractions were pooled, concentrated by ultrafiltration, and then desalted using a HiTrap desalting column (Amersham Pharmacia, Sweden). Protein concentrations were determined using the Bradford method. SDS-PAGE and Western blotting were carried out using standard procedures (*16*).

The molecular mass of the native DHAD was determined by size exclusion chromatography. Purified DHAD (54 μg) was chromatographed at a flow rate of 0.5 ml/min on a Sephacryl S-200 column (1.0 × 89 cm) using a gel filtration calibration kit (Amersham Pharmacia Biotech, Sweden). The buffer used for column equilibrium and elution was 50 mM Tris-HCl (pH 7.2) containing 150 mM NaCl. The molecular weight markers used were thyroglobulin (669 kDa), ferritin (440 kDa), aldolase (158 kDa), BSA (67 kDa), and ovalbumin (43 kDa). The absorbance of the eluent was monitored at 280 nm, and DHAD activity was measured by the semicarbizide method described above.

Enzyme Characterization—DHAD activity was determined by the semicarbazide method that was used for gluconate dehydratase activity (*17*). The reaction mixture with a total volume of 400 μl was incubated at 78°C in 50 mM Tris-HCl buffer (pH 7.0) with 10 mM 2,3-dihydroxyisovalerate and the enzyme solution. After 30 min, the enzyme reaction was stopped by adding 100 μl of 2.0 N HCl. To this solution, 300 μl of semicarbizide solution [1.0% (w/v) semicarbazide hydrochloride and 1.5% (w/v) sodium acetate dissolved in distilled water] was added, and the mixture was incubated at 30°C for 15 min. Finally, the reaction mixture was diluted with 500 μl of distilled water, and its absorbance was measured at 250 nm (extinction coefficient = 0.169 mM^{-1} cm^{-1}). This method could detect quantitatively almost all of the 2-keto-isovalerate and showed linearity in an extended range of concentrations. All enzyme activities were determined in triplicate.

The specificities of a DHAD for a natural substrate and aldonic acids were determined by determining the levels of 2-keto-3-deoxy analogs produced from the aldonic acids. The aldonic acids used in this work were 2,3-dihydroxyisovalerate, L-threonate, D- and L-tartarate, D- and L-arabonate, D-xylonate, D-ribonate, D-fuconate, D-galacturonate, D-glucuronate, D-glucarate, D- and L-mannonate, D-galactonate, D-gluconate, and D-galactoheptonate. The apparent V_{max} and K_m values were calculated by fitting the initial rate data to the Michaelis-Menten equation with the non-linear regression analysis program Sigma Plot (ver. 7.0). To detect 2-keto-3-deoxy-gluconate, samples were withdrawn at different times and analyzed by TLC on silica gel G-60 plates developed with *n*-butanol/acetic acid/water (3 : 1 : 1, v/v/v) (*16*). The solvent was removed, and the plates were sprayed with 25 mM periodic acid in 0.25 N H_2SO_4. After 15 min, a solution consisting of ethylene glycol/acetone/sulfuric acid (50 : 50/0.3) was sprayed onto the TLC plates. When completely dry, the plates were sprayed with 6% 2-thiobarbituric acid and heated at 100°C for 10 min.

The temperature profile of the enzyme activity was determined between 40 and 100°C. The enzyme thermostability was determined at 70, 75, 80, 90, and 100°C by incubating the enzyme in 50 mM Tri-HCl (pH 7.2). At appropriate times, samples were removed and immediately cooled on ice, and then residual enzyme activity was determined by the semicarbazide method. The effect of pH on DHAD activity was determined at 78°C in 50 mM citric acid–NaOH buffer (pH 2.7–6.0), 50 mM Tris-HCl buffer (pH 6.0–8.5), or 50 mM glycine-NaOH buffer (pH 8.8–10.5) using the semicarbazide method.

The effects of divalent ions and EDTA on DHAD were determined by measuring the enzymatic activity after pre-incubation in 50 mM Tris-HCl (pH 7.2) at 30°C for 1 h in the presence of each of these divalent ions. The effects of thiol compounds (glutathione, dithiothreitol, and 2-mercaptoethanol) and thiol modification reagents (iodoacetamide, *p*-chloromercuribenzoic acid, and *p*-hydroxymecuribenzoic acid) on enzyme activity were determined by the semicarbazide method using the same procedure, but substituting these reagents for the divalent ions.

The effects of oxygen and peroxide on DHAD were determined by measuring the enzymatic activity in 50 mM Tris-HCl (pH 7.2) at 30°C over 2 h under aerobic/anaerobic conditions or in the presence of 0.5% hydrogen peroxide and 0.5% cumen hydroperoxide. Aerobic conditions were created in the buffer in a sealed tube by purging with air, and anaerobic conditions were created by purging with nitrogen gas. The enzyme activities were determined by

the semicarbazide method under the same conditions as described above.

RESULTS AND DISCUSSION

Expression and Purification of the Recombinant Enzyme—The expression level of *Sso_ilvD* in *E. coli* was too low to be detected by SDS-PAGE analysis, but a protein band of approximately 66 kDa was revealed on Western blot analysis performed with an anti-His antibody (Fig. 1A). The recombinant enzyme was purified about 20-fold, with a yield of 3.5%, and had a specific activity of 47 U/mg toward 2,3-dihydroxyisovalerate. The purified protein showed a single band on SDS-PAGE with an apparent molecular weight of *ca.* 66 kDa (Fig. 1B), which is close to the calculated molecular mass of the recombinant protein (59.4 kDa DHAD + 4.7 kDa His-tag = 64.1 kDa). The apparent molecular mass of the native protein was determined to be approximately 125 ± 5 kDa, indicating a homodimeric structure similar to that previously reported for the DHAD from bacteria, fungi, and plants (*2–6*).

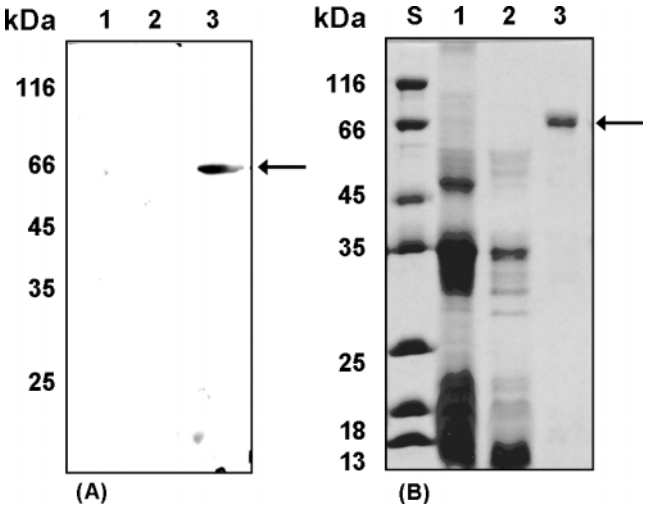

Fig. 1. **Western blot analysis of rSso_DHAD expressed in *E. coli* (A) and SDS-PAGE of the purified rSso_DHAD (B).** (A) lane 1, whole cell lysate of *E. coli* TOP 10; lane 2, whole cell lysate of *E. coli* TOP10 harboring pBAD/His-A; lane 3, whole cell lysate of *E. coli* TOP10 harboring pBAD-Sso_ilvD. (B) S, standard molecular markers; lane 1, crude extract; lane 2, heat-treated crude extract; lane 3, Ni-NTA column eluent.

Substrate Promiscuity in the Recombinant DHAD—Seventeen aldonic acids were tested as substrates for the recombinant DHAD (rSso_DHAD) (Fig. 2). Among the substrates tested, rSso_DHAD showed the highest activity on the natural substrate 2,3-dihydroxyisovaleric acid, which is a tetronic acid. Interestingly, the enzyme also displayed high activity on some pentonic and hexonic acids. The catalytic activity of rSso_DHAD was higher on D-gluconate than on any other sugar acids tested as a substrate. The enzyme activity on D-arabonate and D-xylonate was about 50% of the activity on the natural substrate. In addition, D-galactonate, D-galaturonate, D-glucuronate, and D-fuconate also served as substrates, although the enzyme activities on these acids were less than 30% of that on the natural substrate. On the other hand, no enzyme activity was detected when D-glucarate, D-mannonate, L-mannonate, and D-glucoheptonate were tested as substrates for rSso_DHAD.

To confirm rSso_DHAD activity on D-gluconate, the samples incubated at 37°C, 50°C, and 70°C for various times were analyzed by TLC. After exposure to 6% 2-thiobarbituric acid (*18*), the TLC plates revealed red spots that represented the 2-keto-3-deoxygluconate produced by the enzymatic dehydration of D-gluconate (Fig. 3). As the reaction time increased, the spot intensities

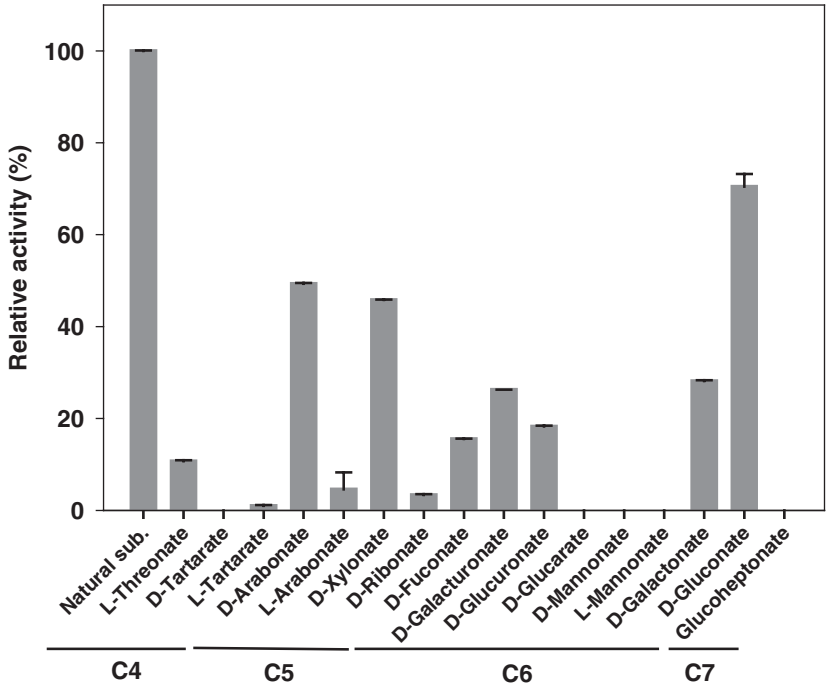

Fig. 2. **Substrate specificity of rSso_DHAD for 17 aldonic acids ranging from four to seven carbon atoms.** The specificities of rSso_DHAD for a natural substrate and aldonic acids were determined by measuring the levels of 2-keto-3-deoxy analogs produced from the aldonic acids using the semicarbazide method.

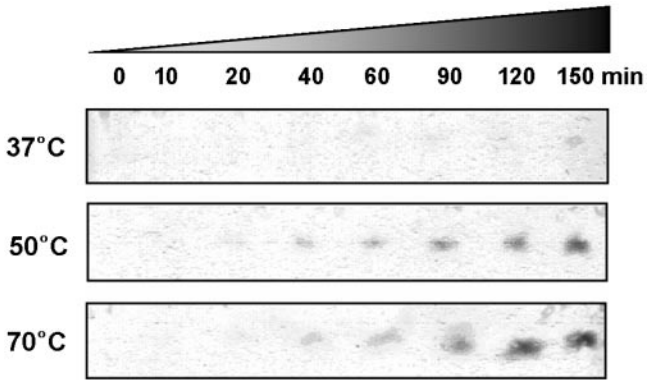

Fig. 3. **Time- and temperature-dependence of the activity of rSso_DHAD on the hexonic acid D-gluconate.** Samples were withdrawn at different times and analyzed by TLC on silica gel G-60 plates developed in *n*-butanol/acetic acid/water. After exposure to 6% 2-thiobarbituric acid, the TLC plates revealed red spots that represented the 2-keto-3-deoxygluconate produced by the enzymatic dehydration of D-gluconate.

from the samples incubated at 50°C and 70°C became greater, whereas no spots appeared in the sample incubated at 37°C. This shows that rSso_DHAD is capable of converting D-gluconate to 2-keto-3-deoxygluconate.

rSso_DHAD showed a classical Michaelis-Menten kinetics pattern on 2,3-dihydroxyisovalerate and D-gluconate. At 70°C, the K_m values of rSso_DHAD were 0.54 mM for 2,3-dihydroxyisovalerate and 2.42 mM for D-gluconate, respectively. Turnover numbers (k_{cat}) were 75.8 s^{-1} for 2,3-dihydroxyisovalerate and 48.5 s^{-1} for D-gluconate, which yielded k_{cat}/K_m values of 140.3 mM^{-1} s^{-1} and 20.0 mM^{-1} s^{-1} for each substrate, respectively.

Other Properties of the Recombinant DHAD—Purified rSso_DHAD showed optimal activity at 80°C, and its activity rapidly decreased at temperatures above 80°C (Fig. 4). The recombinant enzyme was stable at 70°C for over 2 h, whereas its activity was reduced to 50% in 30 min at 80°C. rSso_DHAD showed optimal activity between pH 7.5 and 8.5. DHAD usually requires a metal ion for the enzymatic dehydration of a substrate (*4*, 7, *8*). The activity of rSso_DHAD was enhanced in the presence of Mn^{2+} (160% of control). All of the divalent metal ions tested except Mn^{2+} reduced the enzyme activity: Mg^{2+} (88%), Ca^{2+} (84%), Co^{2+} (30%), Cu^{2+} (15%), Fe^{2+} (12%), Hg^{2+} (9%), Cd^{2+} (6%), Ni^{2+} (3%), Ba^{2+} (3%), and Zn^{2+} (3%).

Several DHAD enzymes purified from bacteria and plants have been shown to require Mn^{2+} or Mg^{2+} for their activities (*8*). rSso_DHAD activity was also increased in the presence of Mn^{2+}. On the other hand, unlike the DHAD of *E. coli* (*1*) and *P. radiatus* (7), the *S. solfataricus* dehydratase was not stimulated by Fe^{2+}. Currently, the mechanisms underlying such a phenomenon remain obscure.

The effect of thiol compounds on the activity of rSso_DHAD was also examined. In the presence of 1 mM glutathione, cysteine, or dithiothreitol, rDHAD activity was greater than 85%, while the enzyme activity decreased to below 60% in the presence of 2-mercaptoethanol. In addition, *p*-hydroxymercuribenzoic acid and *p*-chloromercuribenzoic acid, which modify

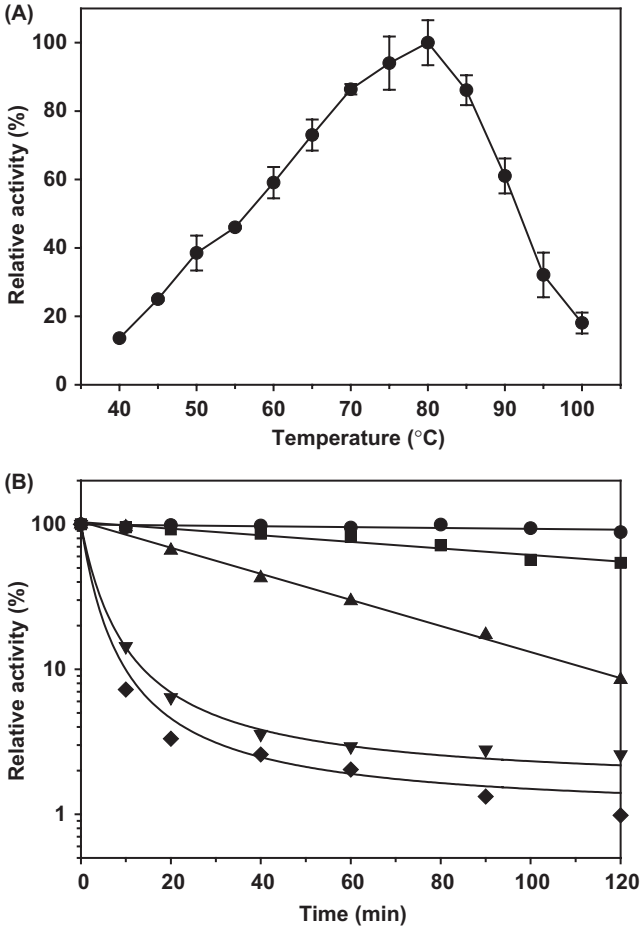

Fig. 4. **Effect of temperature on the activity of rSso_DHAD (A) and thermostability of rSso_DHAD (B).** 70°C (circles), 75°C (squares), 80°C (triangles), 90°C (inverted triangles), 100°C (diamonds).

cysteine residues, strongly inhibited the enzyme activity, whereas iodoacetamide, which acylates thiol groups on proteins, had no effect.

DHADs are known to be oxygen-sensitive enzymes (*2–4*). When rSso_DHAD was incubated in 50 mM Tris-HCl buffer at 30°C for 2 h under aerobic or anaerobic conditions and the residual activity was measured, no difference was found between aerobic and anaerobic conditions. The enzyme was also incubated with organic peroxide under the same conditions. The enzyme activity was stable during exposure to 0.5% organic peroxide for 2 h. In this experiment, rSso_DHAD was not inactivated by oxygen, in contrast to the other DHADs reported previously from bacteria and fungi (*2–6*).

PSI-BLAST searches were performed to examine whether Sso_DHAD contains the cysteine residues which form oxygen-sensitive clusters. Sso_DHAD contains the sequence HXXLGXC (189–195), instead of the oxygen-sensitive CXXCGXC motif found in bacterial DHAD enzymes. In addition, the CXCXXC and CPCXXC motifs, which provide the ligands for [4Fe-4S] clusters and are sensitive to oxygen, were not present in Sso_DHAD. This may explain the differences in the inhibitory effect

of cysteine-modifying reagents and the oxygen sensitivity between Sso_DHAD and other DHADs.

Evolution of DHAD—A database search with Sso_ilvD revealed a large number of sequences with apparent similarity to DHAD and EDD in all three major phylogenic domains of life. Among a total of 85 *ilvD* genes in the COG database (*20*), 36 representative sequences from archaea, bacteria, and eukarya were used for alignments. Interestingly, some DHADs (Cac_ilvD2, Sco_ilvD2, and Sco_ilvD3) are close to the EDD cluster. The phylogenetic tree also shows that the sequences of the archaeal DHADs form two clearly separated domains, Creanarchaeota and Euryarchaeota (Fig. 5): DHADs from the Creanarchaeota cluster close to the eukaryote DHAD and those from the Euryarchaeota cluster close to the bacterial DHAD. This may imply that the bacterial and eukaryotic DHADs evolved from different origins in the ancestral archaea in the early evolutionary stages.

Recently, it has been reported that *S. solfataricus* enzymes possess an unusual promiscuity with respect to substrate and reaction stereospecificity. Currently, three *S. solfataricus* enzymes are supposed to have substrate promiscuity: glucose dehydrogenase, gluconate dehydratase, and 2-keto-3-deoxy-gluconate aldolase (*13*, *14*). Our results indicate that Sso_DHAD is another *S. solfataricus* enzyme which exhibits substrate promiscuity. It is noteworthy that the enzyme involved in the amino acid synthesis can catalyze the conversion of sugar acids such as D-gluconate and D-xylonate to 2-keto-3-deoxy analogs through a similar dehydration reaction. According to the so-called patchwork evolution model, metabolism evolves by the recruitment of relatively inefficient enzymes of

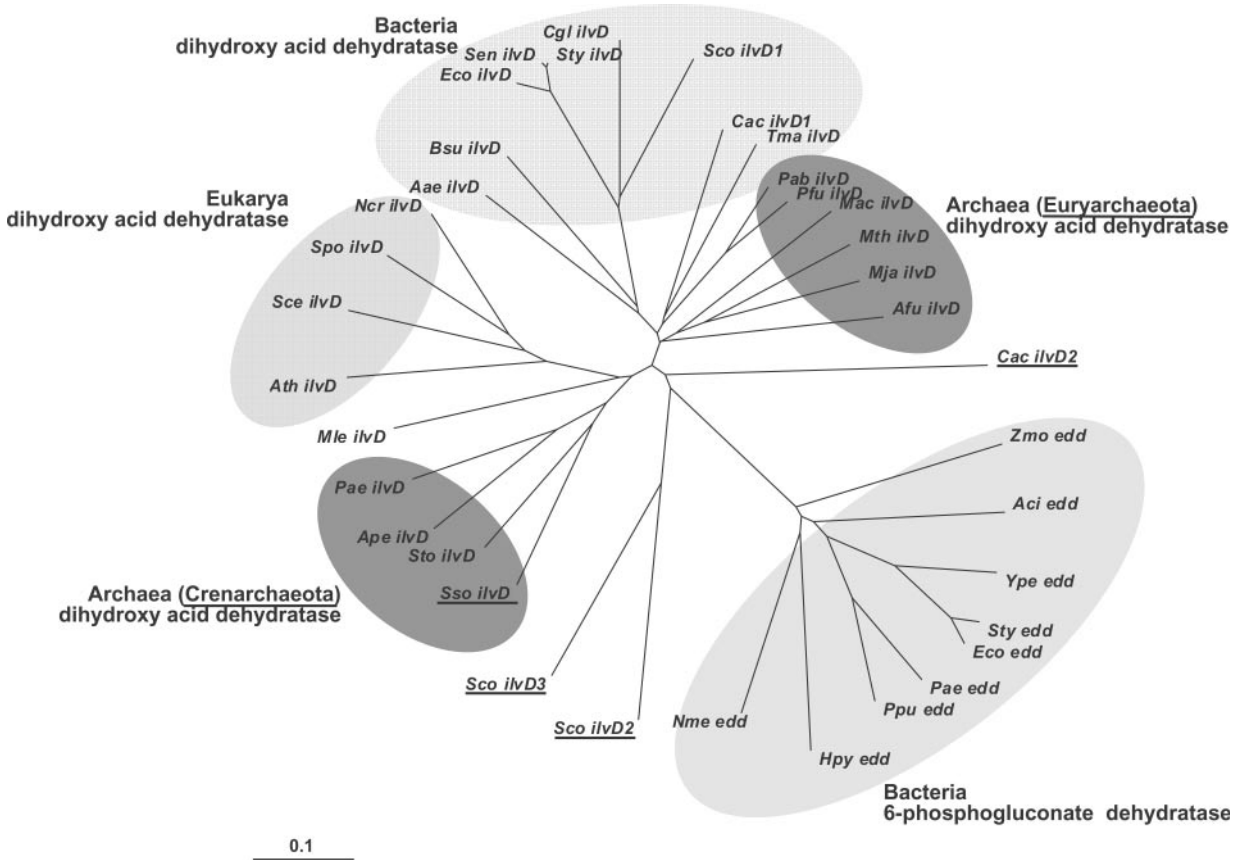

Fig. 5. **Phylogenetic relationship of DHAD and EDD.** The sequence alignments were performed using ClustalW, and the phylogenetic trees were constructed using both the maximum-likelihood and neighbor-joining methods (PHYLIP, version 3.63). The scale bar indicates an evolutionary distance of 0.10 nucleotide per position in the sequence. The abbreviations are as follows. Archaeal DHAD: Sso_ilvD, *S. solfataricus* (GenBank accession number NP_344419); Sto_ilvD, *S. tokodaii* (BAB67277); Ape_ilvD, *A. pernix* (NP_146903); Pae_ilvD, *P. aerophilum* (AAL62897); Pab_ilvD, *P. abyssi* (F75045); Pfu_ilvD, *P. furiosus* (AAL81066); Mac_ilvD, *M. acetivorans* (AAM06742); Mth_ilvD, *M. thermoautotrophicum* (H69059); Mja_ilvD, *M. jannaschii* (NP_248272); Afu_ilvD, *A. fulgidus* (F69376). Bacterial DHAD: Aae_ilvD, *A. aeolicus* (O67009); Bsu_ilvD, *B. subtilis* (D69644); Cac_ilvD1, *C. acetobutylicum* (NP_349767); Cac_ilvD2, *C. acetobutylicum* (NP_350187); Cgl_ilvD, *C. glutamicum* (NP_600490); Eco_ilvD, *E. coli* (AAA67574); Mle_ilvD, *M. leprae* (CAC32140); Sen_ilvD, *S. enterica* (NP_807058); Sco_ilvD1, *S. coelicolor* (NP_627554); Sco_ilvD2, *S. coelicolor* (NP_626154); Sco_ilvD3, *S. coelicolor* (NP_625466); Sty_ilvD, *S. typhimurium* (NP_462795); Syn_ilvD, *Synechocystis* sp. (P74689); Tma_ilvD, *T. maritima* (E72362). Eukaryal DHAD: Ath_ilvD, *A. thaliana* (BAB03011); Ncr_ilvD, *N. crassa* (CAD70774); Sce_ilvD, *S. cerevisiae* (S55205); Spo_ilvD, *S. pombe* (NP_593729). 6-Phosphogluconate dehydratase: Aci_edd, *Acinetobacter* sp. (YP_045290); Eco_edd, *E. coli* (NP_416365); Hpy_edd, *H. pylori* (NP_207891); Nme_edd, *N. meningitidis* (CAB84838); Pae_edd, *P. aeruginosa* (P31961); Ppu_edd, *P. putida* (NP_743171); Sty_edd, *S. typhimurium* (NP_460842); Ype_edd, *Y. pestis* (AAM85223); Zmo_edd, *Z. mobilis* (P21909).

broad specificity that could react with a wide range of chemically related substrates (*22–25*). The results presented in this work appear to support this hypothesis, although it is an open question whether the same enzymes shared the carbohydrate and amino acid pathway in the early evolutionary stages.

This work was supported by a grant from the 21C Frontier Microbial Genomics and Applications Center Program.

REFERENCES

1. Myers, J.W. (1961) Dihydroxy acid dehydrase: an enzyme involved in the biosynthesis of isoleucine and valine. *J. Biol. Chem.* **233**, 1414–1418
2. Arfin, S.M. (1969) Evidence for an enol intermediate in the enzymatic conversion of α,β-dihydroxyisovalerate to α-ketoisovalerate. *J. Biol. Chem.* **244**, 2250–2251
3. Armstrong, F.B., Muller, U.S., Reary, J.B., Whitehouse, D., and Croute, D.H. (1977) Stereoselectivity and stereospecificity of the α,β-dihydroxyacid dehydratase from *Salmonella typhimurium*. *Biochim. Biophys. Acta* **498**, 282–293
4. Xing, R. and Whitman, W. (1991) Characterization of enzymes of the branched-chain amino acid biosynthetic pathway in *Methanococcus* spp. *J. Bacteriol.* **173**, 2086–2092
5. Flint, D.H., Emptage, M.H., Finnegan, M.G., Fu, W., and Johnson, M.K. (1993) The role and properties of the iron-sulfur cluster in *Escherichia coli* dihydroxy-acid dehydratase. *J. Biol. Chem.* **268**, 14732–14742
6. Kanamori, M. and Wixom, R.L. (1963) Studies in valine biosynthesis. V. Characteristics of the purified dihydroxyacid dehydratase from spinach leaves. *J. Biol. Chem.* **238**, 998–1005
7. Satyanarayana, T. and Radhakrishnan, A.N. (1964) Biosynthesis of valine and isoleucine in plants. II. dihydroxyacid dehydratase from *Phaseolus radiatus*. *Biochim. Biophys. Acta* **92**, 367–377
8. Kiritani, K., Narise, S., and Wagner, R.P. (1966) The dihydroxy acid dehydratase of *Neurospora crassa*. *J. Biol. Chem.* **241**, 2042–2046
9. Conway, T. (1992) The Entner-Doudoroff pathway: history, physiology and molecular biology. *FEMS Microbiol. Rev.* **103**, 1–27
10. Egan, S.E., Fliege, R., Tong, S., Shibata, A., and Wolf, R.E. and Conway, T. (1992) Molecular characterization of the Entner-Doudoroff pathway in *Escherichia coli*: sequence analysis and localization of promoters for the *edd-eda* operon. *J. Bacteriol.* **174**, 4638–4646
11. Bender, R. and Gottschalk, G. (1973) Purification and properties of D-gluconate dehydratase from *Clostridium pasteurianum*. *Eur. J. Biochem.* **40**, 309–321.
12. Gottschalk, G. and Bender, R. (1982) D-Gluconate dehydratase from *Clostridium pasteurianum*. *Methods Enzymol.* **90**, 283–287
13. Lamble H.J., Heyer N.I., Bull S.D., Hough D.W., and Danson M.J. (2003) Metabolic pathway promiscuity in the archaeon *Sulfolobus solfataricus* revealed by studies on glucose dehydrogenase and 2-keto-3-deoxygluconate aldolase. *J. Biol. Chem.* **278**, 34066–34072
14. Lamble H.J., Milburn C.C., Taylor G.L., Hough D.W., and Danson M.J. (2004) Gluconate dehydratase from the promiscuous Entner-Doudoroff pathway in *Sulfolobus solfataricus*. *FEBS Lett.* **576**, 133–136
15. Kim, S. and Lee, S.B. (2004) Thermostable esterase from a thermoacidophilic archaeon: purification and characterization for enzymatic resolution of a chiral compound. *Biosci. Biotechnol. Biochem.* **68**, 2289–2298
16. Sambrook, J. and Russell, D.W. (2001) *Molecular Cloning: A Laboratory Manual*, 3rd ed., Cold Spring Harbor Laboratory, Cold Spring Harbor, NY
17. Kim, S. and Lee, S.B. (2005) Identification and characterization of *Sulfolobus solfataricus* D-gluconate dehydratase: a key enzyme in the non-phosphorylated Entner-Doudoroff pathway. *Biochem. J.* **387**, 271–280
18. Warren, L. (1960) Thiobarbituric acid spray reaction for deoxy sugars and sialic acids. *Nature* **186**, 237
19. Henikoff, S. and Henikoff, J.G. (1992) Amino acid substitution matrices from protein blocks. *Proc. Nat. Acad. Sci. USA* **89**, 10915–10919
20. Flint, D.H., Tuminello, J.F., and Emptage, M.H. (1993) The inactivation of Fe-S cluster containing hydro-lyases by superoxide. *J. Biol. Chem.* **268**, 22369–22376
21. Flint, D.H. and Emptage, M.H. (1988) Dihydroxy acid dehydratase from spinach contains a [2Fe-2S] cluster. *J. Biol. Chem.* **263**, 3558–3564
22. Jensen, R.A. (1976) Enzyme recruitment in evolution of new function. *Ann. Rev. Microbiol.* **30**, 409–425
23. Lazcano, A., Diaz-Villagomez, E., Mills, T., and Oro, J. (1995) On the levels of enzymatic substrate specificity: implications for the early evolution of metabolic pathways. *Adv. Space Res.* **15**, 345–356
24. O'Brien, P.J. and Herschlag, D. (1999) Catalytic promiscuity and the evolution of new enzymatic activities. *Chem. Biol.* **6**, R91–R105
25. Macchiarulo, A., Nobeli, I., and Thornton, J.M. (2004) Ligand selectivity and competition between enzymes in silico. *Nat. Biotechnol.* **22**, 1039–1045